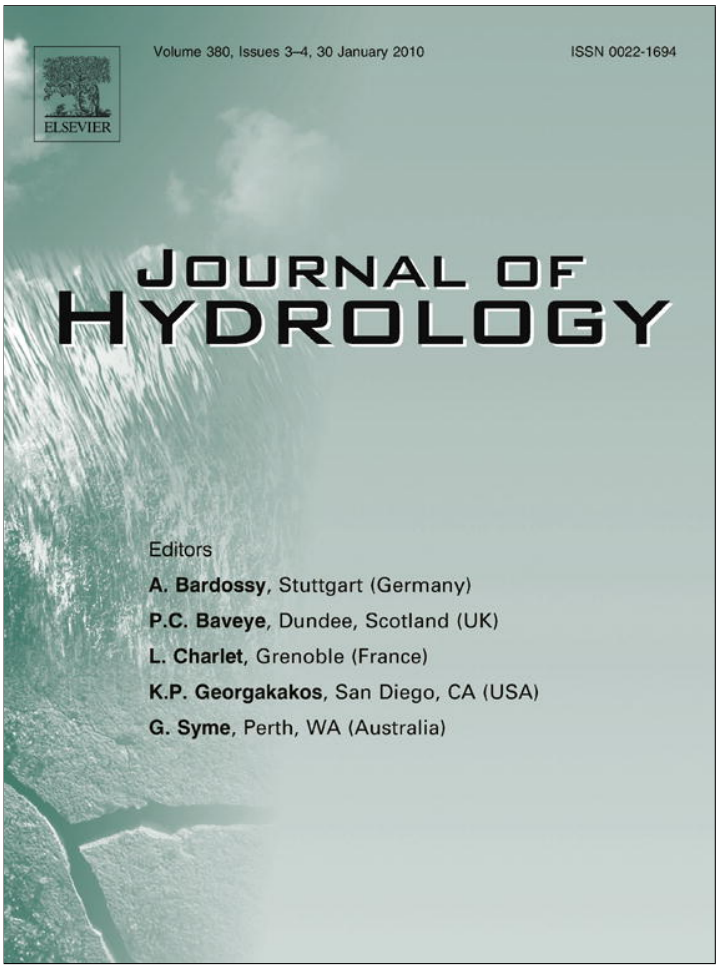

Journal of Hydrology 380 (2010) 438–449

Contents lists available at ScienceDirect

Journal of Hydrology

journal homepage: www.elsevier.com/locate/jhydrol

Climate informed monthly streamflow forecasts for the Brazilian hydropower network using a periodic ridge regression model

Carlos H.R. Lima *, Upmanu Lall

Columbia University, Dept. of Earth and Environmental Engineering, 842 Mudd, 500 W 120th. St., New York, NY 10027, USA

ARTICLE INFO

Article history:
Received 4 April 2009
Received in revised form 1 September 2009
Accepted 8 November 2009

This manuscript was handled by
Dr. A. Bardossy, Editor-in-Chief, with the
assistance of Ercan Kahya, Associate Editor

Keywords:
Climate informed streamflow forecasts
Hydropower reservoirs
Ridge regression
Periodic models

SUMMARY

Streamflow simulation and forecasts have been widely used in water resources management, particularly for flood and drought analysis and for the determination of optimal operational rules for reservoir systems used for water supply and energy production. Here we include climate information in a periodic-auto-regressive model in order to provide monthly streamflow forecasts for 54 hydropower sites in Brazil. Large scale climate information is included in the model through the use of climate indices obtained from the sea surface temperature field of the tropical Pacific and sub-tropical Atlantic oceans and the low-level zonal wind field over southeast Brazil. Correlation analysis of climate predictors and streamflow data show that the dependence of the latter on climate variability is seasonal and also a function of the lead time of the forecasts. A ridge regression framework is adopted in order to shrink parameter estimates and improve model outputs. The proposed model is compared with an ordinary linear regression based model with predictors selected by the BIC criterion and with the classical linear periodic-auto-regressive model (PAR), where no climate information is used. Cross-validated results show that the inclusion of climate indexes is able to improve forecast skills up to 3 months lead time. Higher skills are observed for reservoirs with large catchment areas.

Introduction

The ability to adapt management of water resources systems using climate based forecasts is being highlighted as a key climate change adaptation strategy. This is particularly important for the Brazilian hydropower system which supplies most of the electrical energy for Brazil. With more than 70 interconnected (hydraulically and through transmission lines of electrical energy) hydropower reservoirs that account for approximately 79% of the 91 GW installed capacity (Marreco and Carpio, 2006) in the country, the Brazilian hydropower system needs to use streamflow forecasts (e.g. Costa et al., 2007) and optimization models (e.g. Barros et al., 2003) to produce electrical energy with expected maximum reliability and minimum cost.

Since the 2001 failure in hydroenergy supply that resulted in a significant decline in the GDP growth rate (1.5% in 2001 against 4.4% in 2000, Gomide, 2004), the system's national operator (ONS), has looked for more skillful streamflow forecast models in order to improve the efficiency and reliability of the hydropower system. Recent literature (e.g. Collischonn et al., 2005; Guilhon et al., 2007; Silva et al., 2007; Cataldi et al., 2007) shows that most efforts have been concentrated in the development of dynamical models, where streamflows are predicted using hydrological models (i.e. rainfall–runoff models), which in turn are run using predicted precipitation from general (or regional) circulation models. The limited short term predictability of rainfall from such models has however limited climate informed streamflow forecasts to a few days in advance. Medium and long term (months, years) streamflow forecasts and simulations have been mostly based on the classical periodic-auto-regressive (PAR) class of models (Costa et al., 2003, 2007; Maceira et al., 2005) which do not consider any observed or predicted climate information. These have limited utility in seasons where the temporal persistence in the streamflow process is weak and large-scale climate forcings are important.

More recently, data based and empirical analysis have led to important advances in understanding how large-scale climate anomalies extend to far areas and significantly alter rainfall and streamflow patterns. Statistical models that directly link the hydrological variable of interest (e.g. streamflow) with externals forcings (i.e. climate predictors) have been developed. Those empirical models have been proved to be at least as powerful as physical based models in predicting streamflow and rainfall patterns. Examples of applications can be seen in Uvo and Graham (1998), Kelman et al. (2000), Filho and Lall (2003), Grantz et al. (2005), Maity and Kumar (2008), Kumar and Maity (2008). Here we use climate indexes in a periodic-auto-regressive exogenous

* Corresponding author.
E-mail addresses: chr2107@columbia.edu (C.H.R. Lima), ula2@columbia.edu (U. Lall).

0022-1694/$ - see front matter © 2009 Elsevier B.V. All rights reserved.
doi:10.1016/j.jhydrol.2009.11.016

(PARX) model for monthly flow forecasts. The periodic-auto-regressive component accounts for the seasonally varying persistence of streamflow while external forcings due to climate variability are included in the periodic exogenous part. The inclusion of climate information in PAR models aims to go beyond the persistence terms of the auto-regressive models and reduce the variance of the forecasts. Climate indexes used are obtained from the sea surface temperature (SST) in the tropical Pacific and sub-tropical Atlantic and from the low level (700 mb) zonal wind over south-east Brazil.

Recognizing that the influence and intensity of remote teleconnections changes throughout the year and models with a large number of correlated predictors may lead to high variance in parameters and poor fitting, we use ridge regression (Hastie et al., 2001) in order to shrink the linear model parameters and reduce their variance. Note that periodic auto-regressive exogenous (PARX) modeling is in the domain of regression rather than time series analysis. A comparison is made with the classical linear regression model, where the Bayesian Information Criterion (BIC, see Hastie et al., 2001) is used to select the best set of predictors to be included in the model according to the lead time and month of the forecast. PAR based forecasts are also examined in order to see whether climate information can improve on streamflow forecasts by these traditional models. We evaluate these models using streamflow data from 54 hydropower sites in Brazil. Forecasts are made for up to 6 month lead time. This paper is organized as follows: in the next section we describe the streamflow and climate data. Large scale climate influences on streamflow patterns across Brazil and the climate indexes selected for the forecast model are presented in the section titled "Climate teleconnections and predictors". In the section "Forecast model" we provide the formal description of the forecast model. Finally in the section "Results" we present cross-validated results and a comparison across the tested models.

Hydroclimatic data

Naturalized monthly series of streamflows from 54 hydropower sites in Brazil are provided by ONS. Fig. 1 shows the location of these sites within geographical regions in Brazil as defined in Grimm (2004). The main hydrological basins in Brazil as adopted by the Brazilian National Water Agency (ANA) are shown in Fig. 1. Note that most hydropower reservoirs belong to the Paraná river basin (region 4 in Fig. 1) and are located in the central-east region of the country.

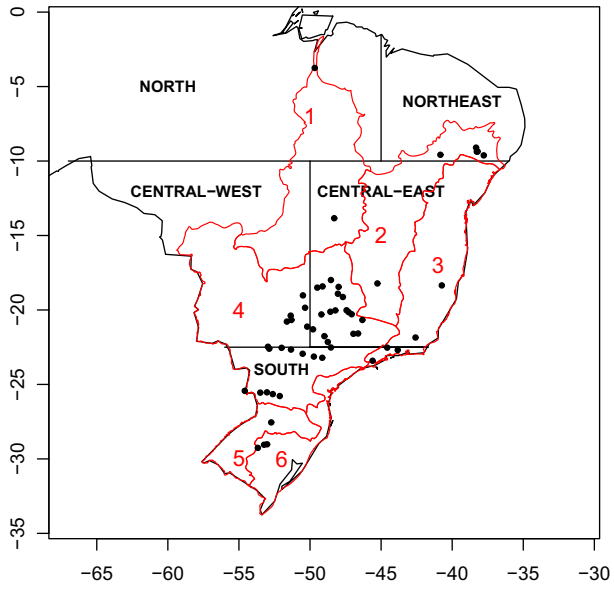

Fig. 1. Location of the hydropower sites used here. The geographical regions (black lines) are defined as in Grimm (2004). The red lines show the geographical delimitation of the main hydrological basins in Brazil as defined by the National Water Agency (ANA): 1 – Tocantins; 2 – São Francisco; 3 – Atlântico Leste; 4 – Paraná; 5 – Uruguai and 6 – Atlântico Sudeste.

The streamflow series covers the 1949–2006 period and does not have any missing values. Catchment areas range from 322 to 823,555 km^2. A consolidation and consistency process is used by ONS to obtain the naturalized flows from artificial and natural streamflow gauges. Reservoir operations upstream of the streamflow gauge are removed from the original series whereas evaporation from the hydropower reservoir and water withdraws across the reservoir basin are estimated and added to the original series. Some streamflow gauges are atypical and involve pumping, transpositions between river and canals, bypasses, etc, adding more complexity to the consistency process. More details can be found in ONS (2007).

Interpolated data of sea surface temperature (SST) anomalies from the Tropical and Atlantic oceans (Kaplan et al., 1998; Reynolds and Smith, 1994) are provided by the International Research Institute for Climate and Society (IRI) and available at http://iridl.ldeo.columbia.edu/SOURCES/.KAPLAN/.EXTENDED/.v2/.ssta/. The NOAA NCEP-NCAR Reanalysis data of low level (700 mb) zonal wind data is available at http://www.iridl.ldeo.columbia.edu/SOURCES/.NOAA/.NCEP-NCAR/.CDAS-1/.MONTHLY/.Intrinsic/.PressureLevel/.u/. Both data sets cover the same period of the streamflow data.

Climate teleconnections and predictors

Rainfall and streamflow patterns across Brazil are mainly affected by SST from three distinct regions: (i) Tropical Pacific Ocean, associated with El Niño and La Niña events (Ropelewski and Halpert, 1987; Grimm et al., 1998; Cardoso and Dias, 2006; Lima et al., 2006); (ii) sub-tropical Atlantic Ocean accompanying by changes in the south Atlantic convergence zone (SACZ) (Barros et al., 2000; Carvalho et al., 2004; Lima and Lall, 2008) and (iii) Tropical Atlantic Ocean combined with the displacement of the inter-tropical convergence zone (ITCZ) (Moura and Shukla, 1981; Hastenrath, 1994). For the purposes of this work, the first two teleconnections are more important, since the latter is most associated with changes in rainfall patterns over Northeast Brazil and the Amazon region, where few hydropower reservoirs are installed.

Rainfall and streamflow pattern changes associated with El Niño events

Global impacts of El Niño events are well documented (see for instance Diaz and Markgraf (2000) and references therein). In Brazil, El Niño events usually lead to a *dipole* pattern of rainfall, drier conditions in Northeast Brazil during the austral spring and summer and consistent wetter conditions in southern Brazil in the austral spring mainly (Ropelewski and Halpert, 1987; Grimm et al., 1998). Particularly, the enhancement of rainfall over the southern region has been associated with stronger than normal 200-hPa subtropical westerly jets during El Nino events, which in turn favor the intensification of mesoscale convection centers in south Brazil. It also displaces an anomalous anti-cyclonic circulation southeastern of Brazil and a cyclonic anomaly southwest of South America that favor baroclinic instabilities and anomalous rainfall patterns in south Brazil (Ropelewski and Halpert, 1987; Cardoso and Dias, 2006; Coelho et al., 2002; Diaz and Markgraf, 2000; Grimm, 2004; Grimm et al., 2000, 1998). Grimm (2004, 2003) also concluded that the effects of ENSO on the rainfall over the central-east

region tend to be smoothed out on a seasonal analysis basis and show that the region experiences positive (negative) rainfall anomalies mostly in January following an El Niño (La Nina) event.

Fig. 2 shows lagged correlations between the NINO3 index, defined as the monthly mean sea surface temperature (SST) anomaly (with annual cycle removed) averaged over the geographical area 5°N–5°S latitude, 150°W–90°W longitude, and streamflow data for March and September. Lima et al. (2007) findings show that peak flow of the wet season and the minimum dry season flow of most hydropower reservoirs in Brazil (except those located in south Brazil) take place on average during these months. For the hydropower reservoirs in southern Brazil, March and September are months of below and above average flow, respectively. The positive correlations observed for both seasons indicate that during El Niño events wetter conditions prevail in both seasons, but statistically significant correlations appear more frequently during the dry season. Note also that the March flows of roughly the same number of reservoirs in the central-east and south regions are affected by the February NINO3 index (top left panel in Fig. 2). A similar plot (not shown here) for January shows that significant correlations with the December NINO3 index appear only for reservoirs located in the central-east and central-west regions, agreeing with previous findings (Grimm, 2004, 2003) that show the affect of intra-seasonal changes in the El Niño on rainfall patterns across Brazil.

The south Atlantic convergence zone (SACZ)

The austral summer rainfall over central, southeast and south Brazil is associated with the SACZ, which results from a circulation pattern of winds and moisture similar to the circulation of monsoon systems. The south Atlantic subtropical high and the continental (south Brazil and Argentine) low pressure center induce a continental scale gyre responsible for the moisture transport from the Atlantic Ocean to the Amazon region and then further southward to the subtropics and midlatitudes of South America (Carvalho et al., 2004; Vera et al., 2006).

The SACZ is characterized by *a northwest–southeast-oriented band of maximum rainfall extending off the southeast coast into the south Atlantic* (Lenters and Cook, 1995). Precipitation along this zone is driven by pulses of latent heat from the Amazon basin, by orographic effects of the Andes mountains and by SST anomalies (Lenters and Cook, 1995; Figueroa et al., 1995; Berbery and Collini, 2000). Enhancements in the SACZ have resulted in flood events in southeast and part of south Brazil (Lima and Lall, 2008) and have also been associated with El Niño events (Liebmann et al., 1999; Barros et al., 2000; Carvalho et al., 2004).

Acknowledging the effect of the sub-tropical Atlantic SST and moisture transport on rainfall and streamflow patterns in Brazil, we consider here, in addition to the NINO3 index, two other climate predictors, obtained from a correlation analysis of the south

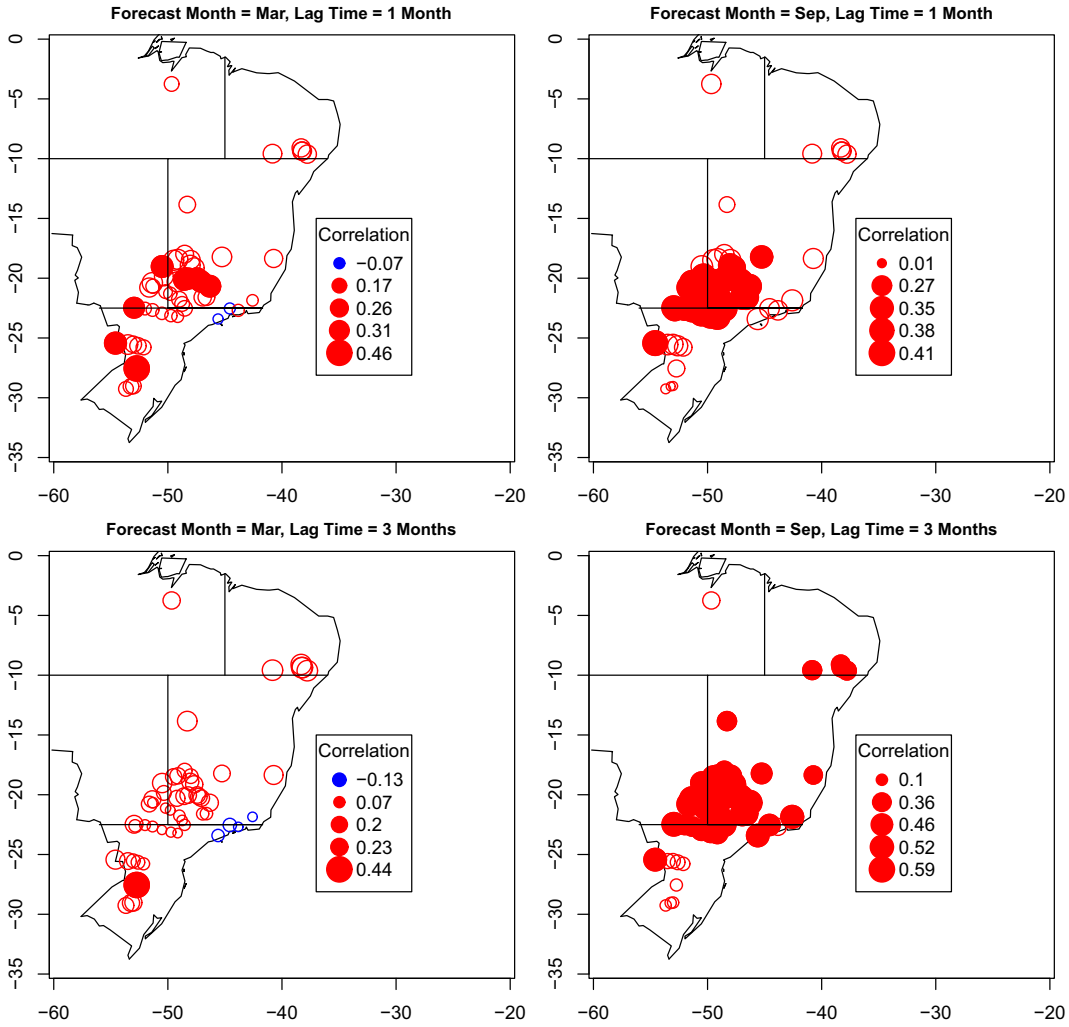

Fig. 2. Lagged correlations between March and September flows and the NINO3 index. Solid circles show correlations that are statistically significant at the 5% significance level. The labels for the geographical regions across the country (black lines) are shown in Fig. 1.

Atlantic SST and low-level zonal wind data with the inflow of the Sobradinho hydropower reservoir, which is located in southern Northeast Brazil, just above the SACZ band. Correlation maps between response variable and climate predictors are analyzed (not shown here) and the regions of high correlations are identified. The climate predictors are obtained by spatially averaging the climate variable of interest (SST or zonal wind) over the region of highest correlations. The first climate index is obtained by averaging the SST anomaly over the region 12°S–30°S latitude, 40°W–20°W longitude. The second index results from averaging the low level (700 mb) zonal wind over 10°S–20°S latitude, 50°W–35°W longitude. Fig. 3 shows the spatial location of the climate indexes obtained.

Lagged correlations of the south Atlantic SST index and streamflows show (Fig. 4) seasonal patterns of correlation. During the wet season (March), a somewhat *seesaw* structure is observed, where streamflow sites located above ~22°S latitude are negatively correlated with the south Atlantic index, whereas sites below this latitude are positively correlated. This finding is consistent with the literature (Barros et al., 2000; Carvalho et al., 2004; Nogués-Paegle

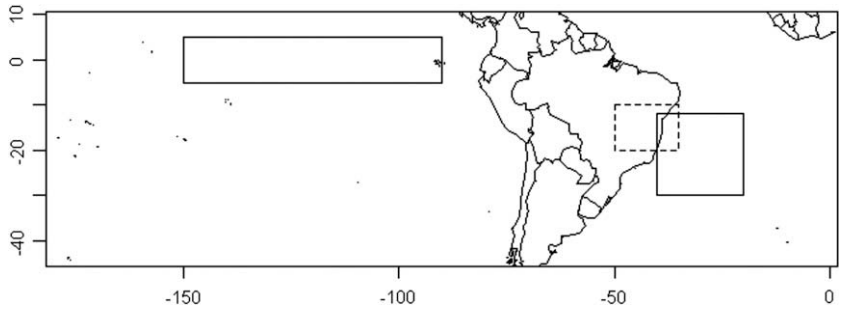

Fig. 3. Spatial location of SST (rectangles with solid line) and low level zonal wind (rectangle with dashed line) based climate indexes.

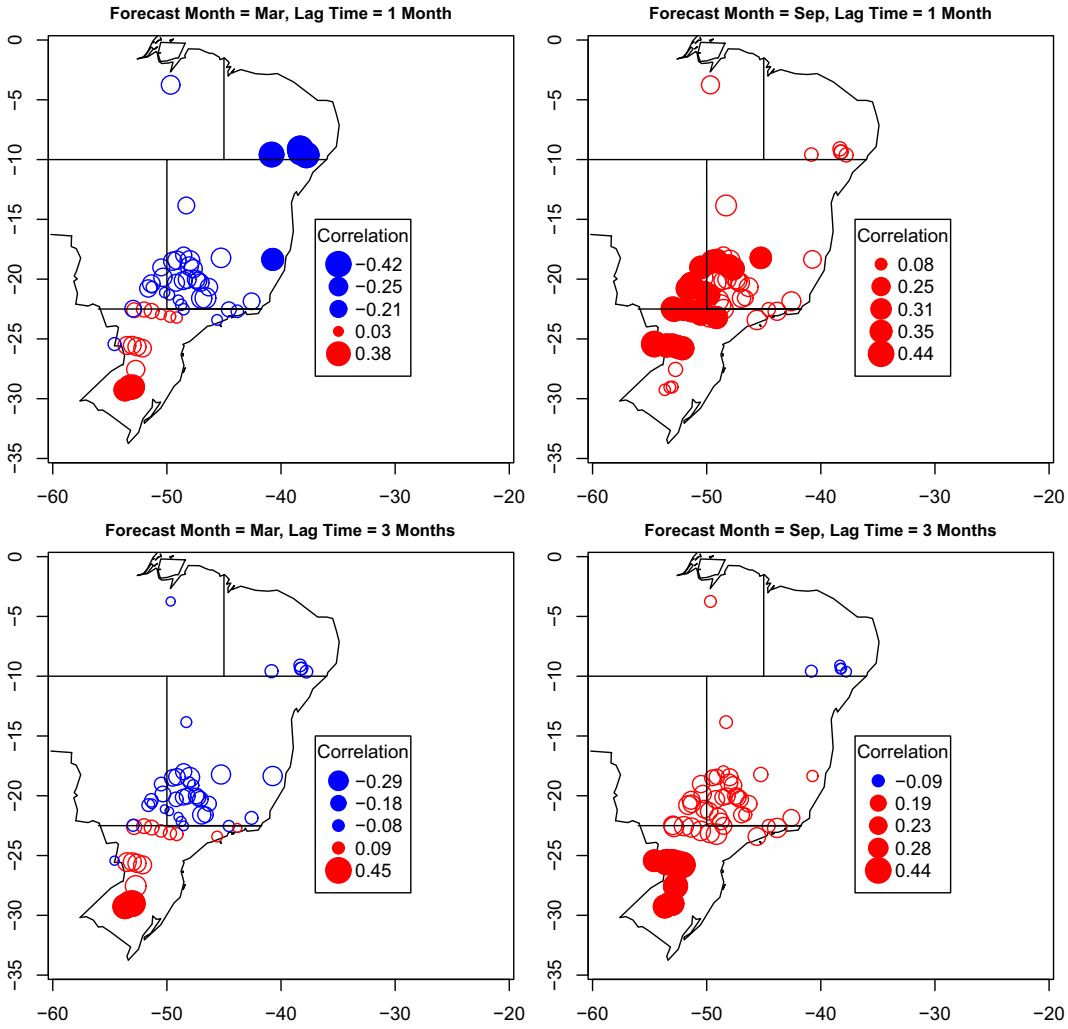

Fig. 4. As in Fig. 2, but for the south Atlantic climate index.

and Mo, 1997; Lima and Lall, 2008), which showed that strong (weak) convection in the SACZ leads to abundant (scarce) rainfall in a band extending from Amazon to south Atlantic and scarce (abundant) rains in Argentine, Chile and south Brazil. Negative anomalies in the south Atlantic SST can be responsible for enhancing the south Atlantic subtropical high and consequently for intensifying the SACZ. On the other hand, positive anomalies of the south Atlantic SST might further decrease the already weak dry season SACZ and favor high flows in most reservoirs.

The lagged correlations of streamflow and the zonal wind index displayed in Fig. 4 show a similar structure as observed for the correlation map with the south Atlantic SST index. Positive anomalies in the zonal wind, whose long term mean in the selected region (Fig. 3) is westward, are associated with an enhancement of the SACZ and consequently with more rainfall in the regions discussed above.

Finally, the at-site periodic auto-correlation function shows (Fig. 5) that persistence is indeed an important term to model the streamflow process, in particular during the dry period.

Forecast model

Let $q(t)$ be the at-site streamflow of month t at an unspecified year. The teleconnection patterns explored in the previous section allow us to model the streamflow process as a function of persistent and exogenous terms:

Table 1
Summary of streamflow forecast models tested here.

Model	Description	Abbreviation	Refer to equation
1	Linear periodic-auto-regressive	PAR	(2) Omitting climate predictors
2	Linear, periodic-auto-regressive exogenous with predictors selected using BIC	PARX	(2)
3	Ridge periodic-auto-regressive exogenous	RIDGE	(2), (4) and (5)

$$q(t) = f(q(t-\tau), x_1(t-\tau), x_2(t-\tau), x_3(t-\tau)) \quad (1)$$

where τ is the lag time and x_1, x_2 and x_3 refer, respectively, to the NINO3, south Atlantic SST and low-level zonal wind indexes, respectively. Typically we vary τ from 1 to 6 months.

A common approach to model the relationship expressed in (1) is to consider f a linear function and $q(t)$ a random variable normally distributed with predictors and seasonally varying parameters:

$$q(t) \sim N(\beta_{0t} + \beta_{1t} q(t-\tau) + \beta_{2t} x_1(t-\tau) + \beta_{3t} x_2(t-\tau) + \beta_{4t} x_3(t-\tau), \sigma_t^2) \quad (2)$$

Since correlated predictors in (2) may increase the variance σ_t^2 (or the uncertainty) of the predictions, a variable selection procedure (Hastie et al., 2001) is usually adopted in order to select a sub-

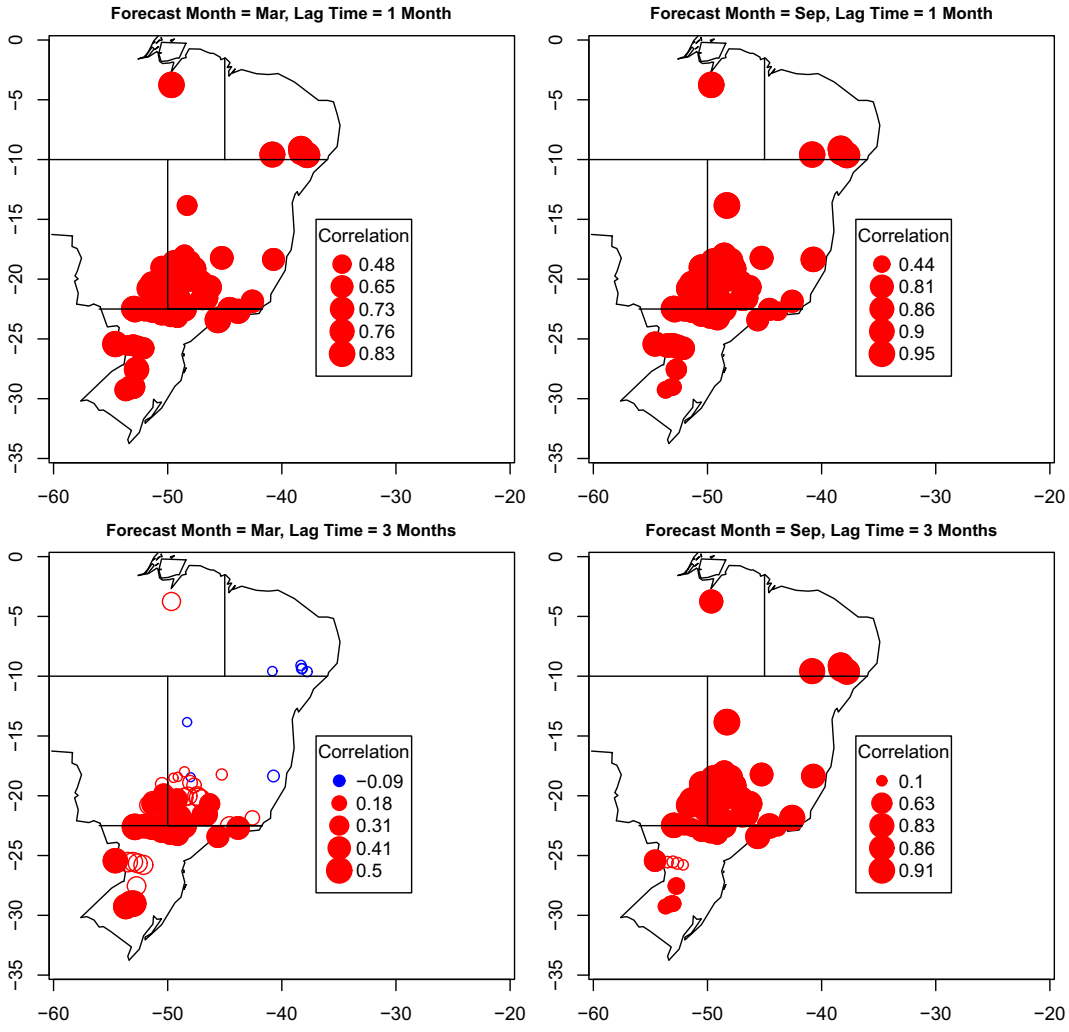

Fig. 5. At-site periodic (for March and September) auto-correlation function for lags 1 and 3 months.

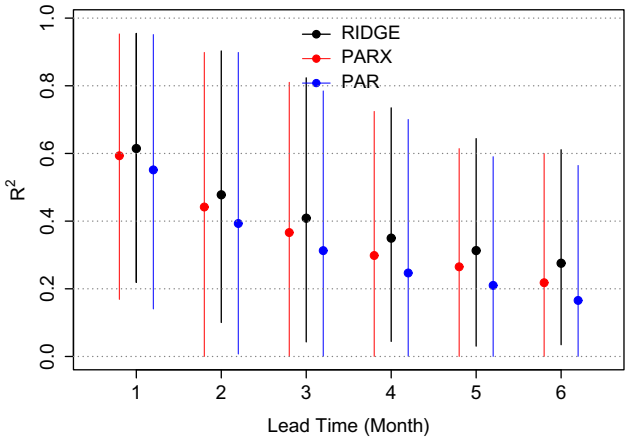

Fig. 6. Range (95% interval) for the coefficient of determination R^2 (vertical bars) as a function of lead time and model tested. The filled circles show the average R^2.

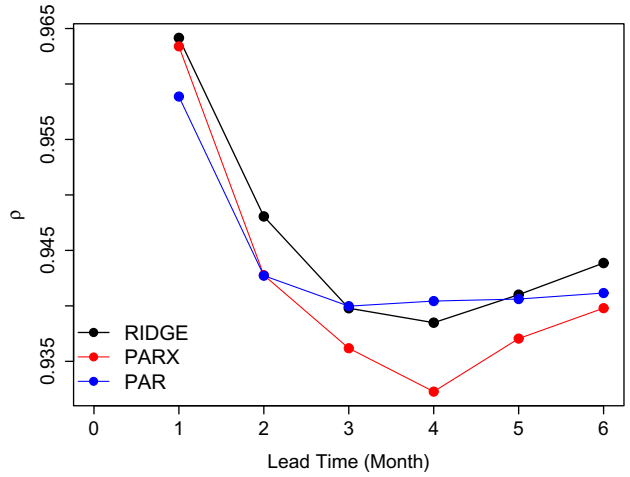

Fig. 7. Pearson correlation coefficient ρ as a function of lead time and model tested.

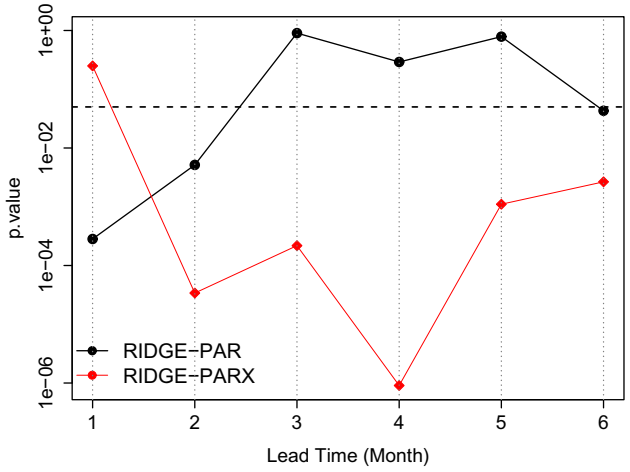

Fig. 8. p-Value for the Diebold–Mariano statistic test under the null hypothesis that the mean squared errors from the two competing model (RIDGE-PAR and RIDGE-PARX) streamflow forecasts are equal (i.e. a 2-sided test). The horizontal dashed line shows p-value = 0.05.

set of predictors in (2) that will potentially lead to the lowest prediction error. Here we use the Bayesian information criterion (BIC), mathematically defined as (Hastie et al., 2001):

$$\mathrm{BIC} = -2 \cdot \log(L) + (\log N) \cdot d \tag{3}$$

where L refers to the maximized likelihood function, N is the number of data points and d the number of free parameters.

The BIC criterion tends to balance the increase in the likelihood of the data and the variance added as the number of parameters included in the model increases. Note that one set of regression parameters is estimated for each reservoir, month and lead time of forecast.

Ridge regression

The BIC procedure adopted here to select the best set of predictors to keep in (2) may still lead to high prediction errors when the selected predictors are highly correlated. Shrinkage methods provide a useful way to constraint the size of the estimates and prevent this to occur. Here we use the ridge regression (Hastie et al., 2001), where the regression parameters in (2) are now calculated as follows:

$$\hat{\beta}_t^{\mathrm{ridge}} = \mathrm{argmin}_\beta \left\{ \sum_{i=1}^{N} (q_i(t) - f_i(x,t))^2 + \delta \sum_{j=1}^{4} \beta_{jt}^2 \right\} \tag{4}$$

where δ is an extra parameter (the "ridge parameter") that determines the shrinkage of the parameters β_{jt}.

The optimal estimate for the ridge regression parameters can be written in matrix form as:

$$\hat{\beta}^{\mathrm{ridge}} = (\mathbf{X}^T\mathbf{X} + \delta\mathbf{I})^{-1}\mathbf{X}^T\mathbf{q} \tag{5}$$

where $\mathbf{X}$ is the centered matrix of inputs and $\mathbf{I}$ the identity matrix. Note that the problem reduces to ordinary least squares when $\delta = 0$.

In the context of Bayesian analysis, ridge regression parameters can be seen as a posterior mean, when one assumes that the prior distributions for the parameters are independent, normal distributions with mean zero and variance τ^2. In this case, $\delta = \frac{\sigma^2}{\tau^2}$, where σ^2 is given in (2) and assumed known (Hastie et al., 2001).

The optimal value for δ for each forecast model is obtained after evaluating the generalized cross-validation error (Hastie et al., 2001) over a range of values for δ (from 1 to 100 in this case) and picking up the value which produces the lowest error.

Results

The streamflow and climate predictors data are first divided into a training set (covering the 1949–1984 period), where model parameters are estimated, and a testing set (1985–2004), where model skills are assessed. A simple statistical analysis (not shown here) reveals that in both periods all reservoirs experienced a variety of streamflow conditions (normal, below normal and above normal). Therefore, it is expected that this choice of training and testing sets minimizes the dependence of the model skills and parameter estimates on the fitting period.

In addition to the two models described above, we also evaluate the performance of a periodic-auto-regressive model, which considers only the intercept and persistence term in (2). Skills of all models are compared with the skill produced by a constant periodic mean model, with the long term mean estimated using the training set data. Table 1 summarizes the models evaluated here.

The coefficient of determination R^2 (Fig. 6) is the metric used to assess the fitting statistics. As one would expect, as the lead time of the forecast increases the skills of the forecast models tend to decrease and the proportion of the training data variance that is accounted for the models described in Table 1 is progressively reduced. For all lead times the RIDGE model shows the highest R^2, ranging from 0.61 for lead time equals to 1 month to 0.27 for 6 month lead.

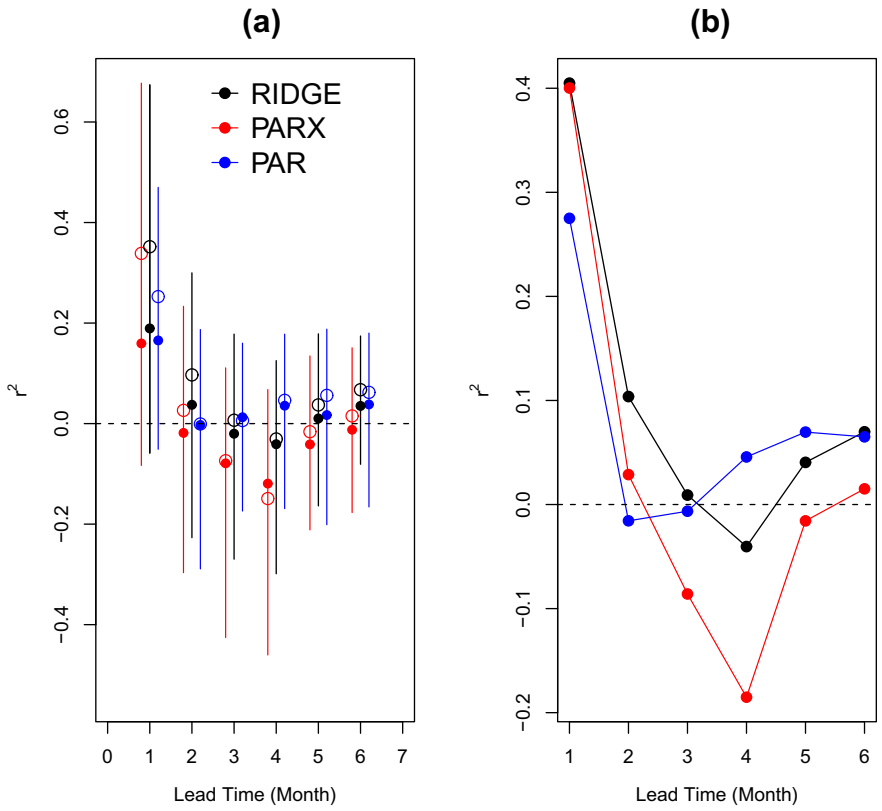

Fig. 9. (a) Range (95% interval) of r^2 scores (vertical bars) as a function of lead time and model tested. Average (filled circles) and catchment area weighted average (open circles) r^2 scores. (b) Average r^2 score for the streamflow sites with the 10 largest drainage areas.

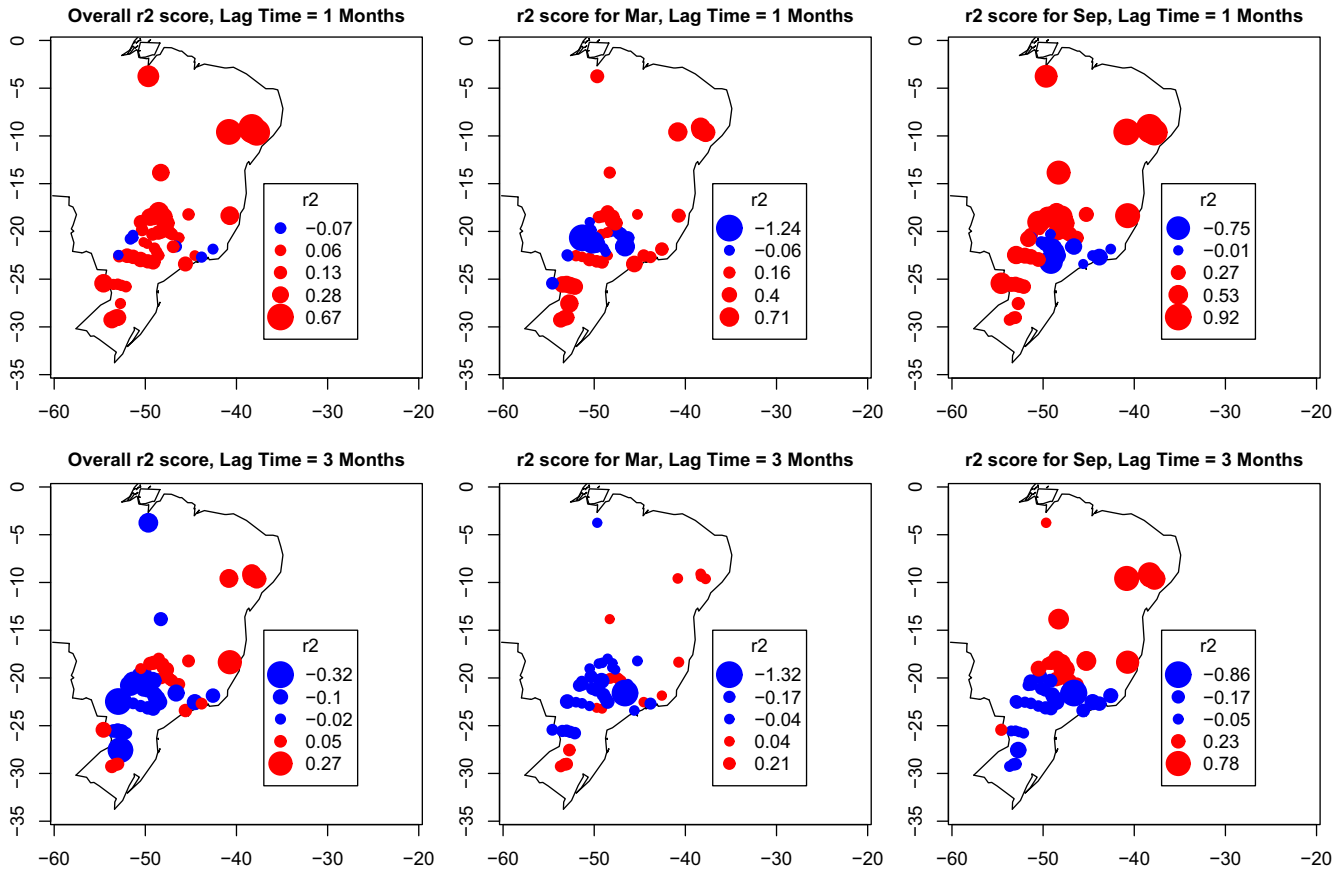

Fig. 10. Spatial distribution of RIDGE model r^2 scores for 1 and 3 month lag times.

In order to evaluate model forecast skill, we compute the Pearson correlation coefficient ρ between observed data and forecasts for the testing set. We calculate ρ across the streamflow series of all reservoirs and their respective forecasts. Fig. 7 shows ρ as a function of lead time and model tested. For the two climate informed forecast models, namely PARX and RIDGE models, the correlation curves resemble a convex function, with a minimum value at 4 month lead time and a subsequent increase in the value thereafter. This recovery in the skill is briefly discussed in "Skill recovery". The PAR correlation curve has an asymptotic behavior, with nearly constant values beyond 3 month lead. Clearly the inclusion of climate information improves streamflow forecasts up to 2 month lead times, as evidenced by the higher correlation from PARX and RIDGE models over the PAR model. Due to the recovery in the skill, the RIDGE model also presents better correlations for lead times of 5 and 6 months. Similar results arise from the plot of the mean squared error statistics (not shown here).

In order to check whether or not the differences among the skills of the three tested models (Fig. 7) are due to sampling error, we test the null hypothesis of equal forecast accuracy of the RIDGE and PARX models and of the RIDGE and PAR models using the Diebold–Mariano test statistic (Diebold and Mariano, 1995). In particular, we test the hypothesis that the mean squared forecast errors of the testing set from the two competing models are equal. For moderately large sample sizes, the Diebold–Mariano test is robust to a wide variety of error distributions, including auto-correlated, heavy-tailed, non-zero mean and contemporaneous forecast errors, when the errors from the two methods are correlated. The test statistic is based on the mean and the variance of the difference between the forecast squared error of the two competing models, in which the estimation of the variance accounts for the serial correlation (reducing then the degrees of freedom) of the forecast error according to the lead time of the forecast. Diebold and Mariano (1995) showed that the asymptotic distribution of this statistic is a standard normal distribution. The p-value for a two-tailed test is shown in Fig. 8 as a function of lead time. When comparing the RIDGE and PAR models (black line in Fig. 8), we reject the null hypothesis of no difference between their forecasts at the 5% level for leads 1, 2 and 6 months, and conclude that the difference between the forecast accuracy of the two models is statistically significant at those leads. Since the correlation coefficient of forecasts and observed values is inversely proportional to the mean squared error, we can conclude from Fig. 7 that this difference is due to the higher skill of the RIDGE model over the PAR model at these leads. Likewise, the difference in the skill of these two models between 3 and 5 month leads is not statistically significant. Finally,

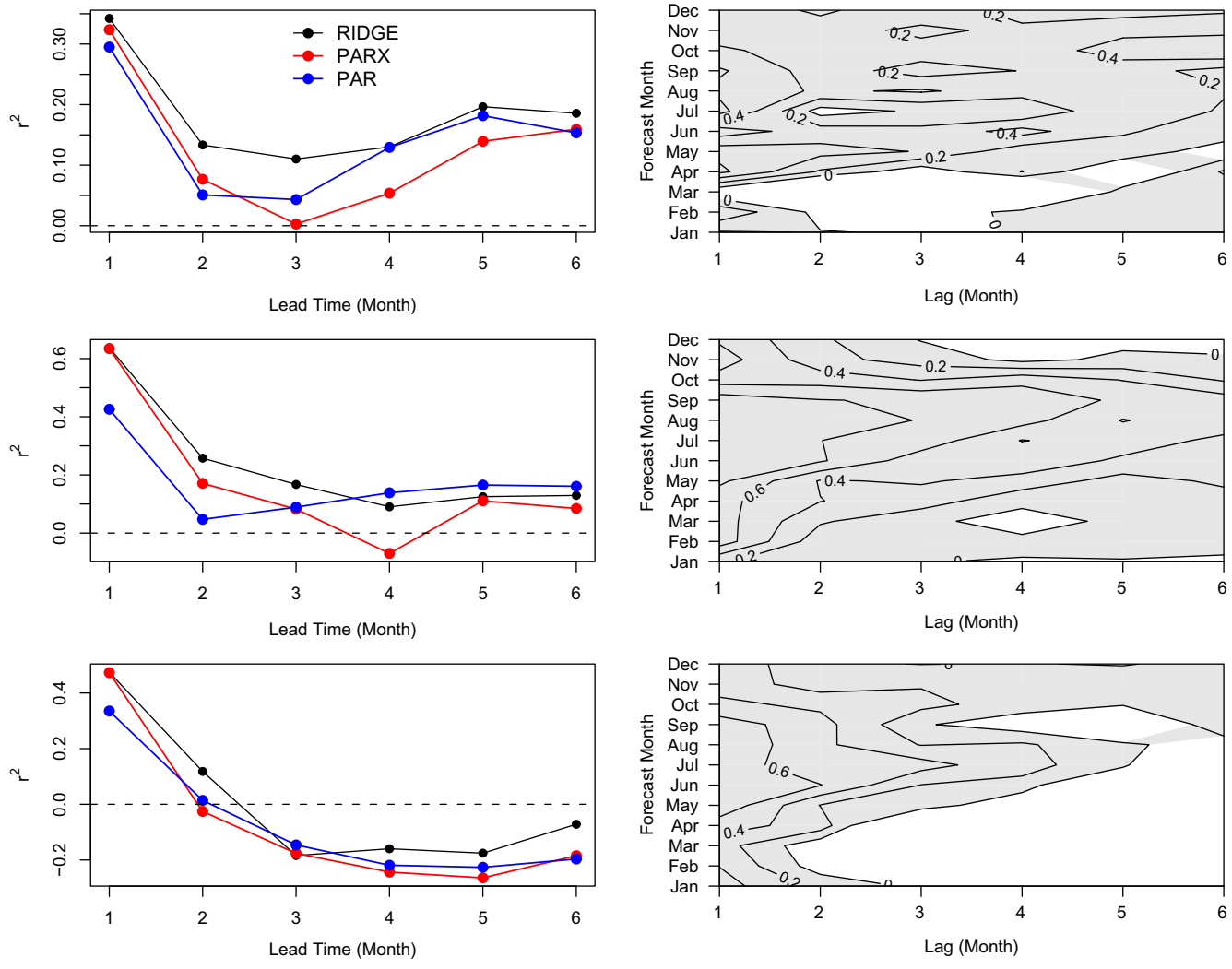

Fig. 11. Left panels: r^2 scores as a function of model and lead time of the forecast for Itaipu (top), Sobradinho (middle) and Tucuruí (bottom) hydropower reservoirs. Right panels: RIDGE model r^2 scores as a function of forecast month and lag time τ of predictors used in the forecast model for the same reservoirs as in the left panel. Gray shaded regions shows $r^2 > 0$.

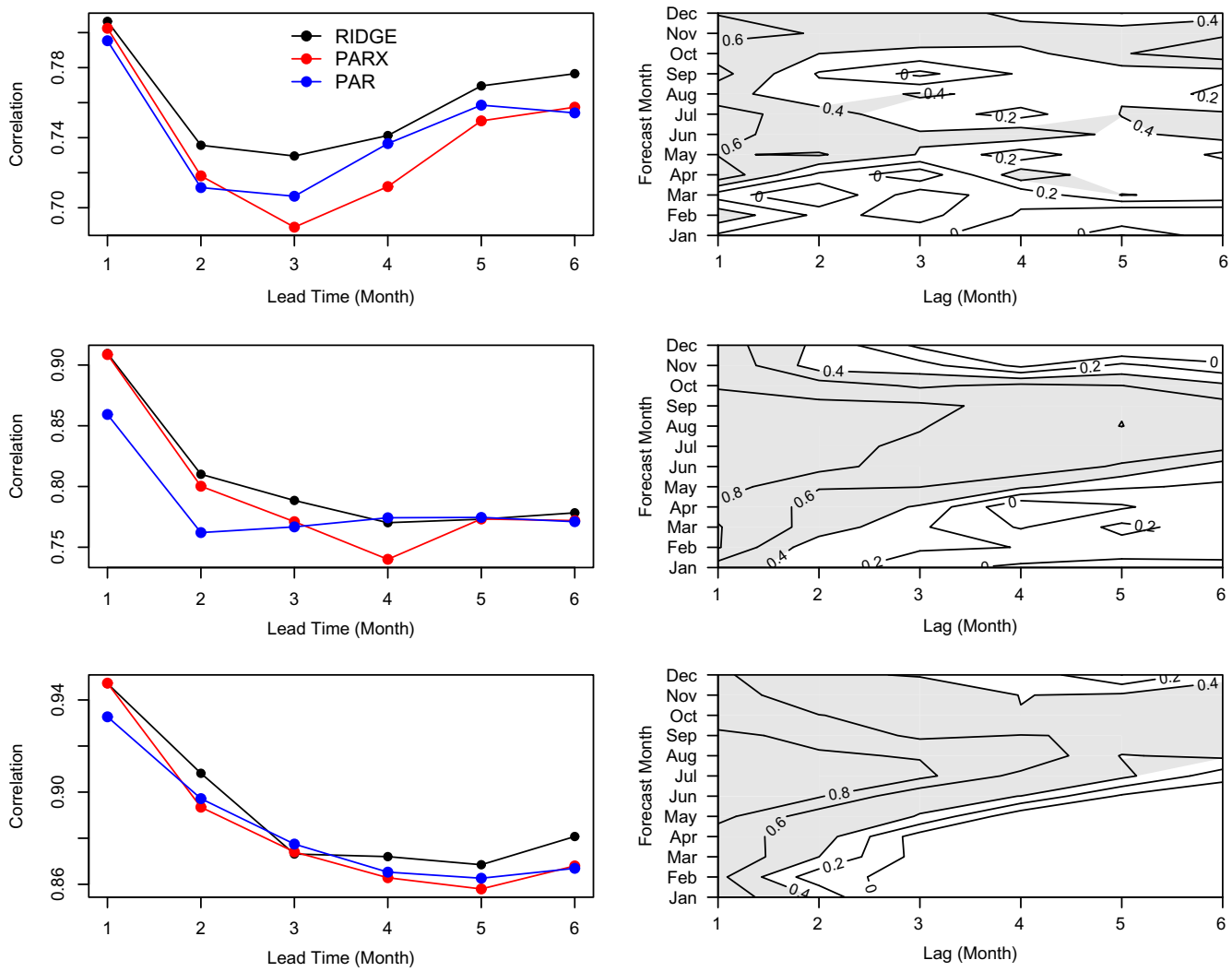

Fig. 12. As in Fig. 11, but for the correlation skill. Gray shaded regions in the right panels show correlations greater than 0.4, which are statistically significant at the 5% significance level.

Fig. 8 (red line)[1] along with the results from Fig. 7 show a statistically significant difference between the PARX and RIDGE model skills in favor of the RIDGE model for all lead times but 1 month lead.

A second criterion used here to evaluate and compare model skills is through the r^2 score (or the Nash–Sutcliffe coefficient), which allows to measure the changes in the forecast skills as one adds persistence and climate predictors into the periodic mean model. The r^2 score for a specific forecast model, lead time of forecast and streamflow site is defined as:

$$r^2 = 1 - \frac{\sum_{t=1}^{12}\sum_{i=1}^{N}(\hat{q}_i(t) - q_i(t))^2}{\sum_{t=1}^{12}\sum_{i=1}^{N}(\bar{q}_i - q_i(t))^2} \quad (6)$$

where $\hat{q}_i(t)$ is the streamflow forecast made by the tested model for month t of year i, $q_i(t)$ is the observed streamflow, $\bar{q}_i$ is the long term average monthly flow based on the 1949–1984 period and N is the total number of years in the record. Note that r^2 has a range of $-\infty$ to +1, and whenever $0 < r^2 \leqslant 1$ the tested model performs better than the simplest possible model based on the long term average.

Fig. 9a displays the r^2 score for each model tested as a function of lead time of forecast. For 1 month lead, the r^2 score ranges (vertical bars in Fig. 9a) for the two models that include climate information are similar and with upper tail values bigger than those from the PAR model. The average r^2 (solid circles) is slightly higher for the RIDGE model. At 2 month lead, on average all models but RIDGE tend to produce forecasts that are no better than the use of the long term mean flow as prediction. As the lead time increases, the PARX model completely lose its forecast skills. The PAR model still performs better than the periodic mean model. At leads 5 and 6 months the PAR and RIDGE models perform similarly. The average r^2 scores (open circles) weighted by the reservoir drainage area show higher values in favor of the RIDGE model up to 3 month lead.

Skills for the hydropower reservoirs with the 10 largest catchment areas are shown in panel 9b. Together, the power capacity of these reservoirs accounts for 65% of the total hydropower capacity in Brazil. At 1 and 2 month leads, the inclusion of climate information significantly improves model forecasts over persistence and long term average based models. At lead two the best skill is achieved by the RIDGE model, which is also able to make forecasts better than the periodic mean model at 3, 5 and 6 month leads.

Spatial distribution of r^2 scores from the RIDGE model at 1 month lag time (top panel in Fig. 10) shows clusters of low predictability reservoirs in the transition region between central-east and south Brazil (between 18°S and 25°S latitude). As the lag time

[1] For interpretation of color in Figs. 8, 13 and 14, the reader is referred to the web version of this article.

increases to 3 months (bottom panel in Fig. 10), one achieves high predictability for the March flow of reservoirs located in northeast and south Brazil whereas the September flow is more predictable for those reservoirs in northeast and part of central-east Brazil. Note also that the differences between March and September r^2 scores are more evident at 3 month lag.

Case study: forecast skills for Itaipu, Sobradinho and Tucuruí hydropower reservoirs

Itaipu, Sobradinho and Tucuruí are the most important reservoirs in Brazil for hydroelectricity generation, hence are the ones in which skilfully streamflow forecasts are more needed. The Itaipu reservoir, which is part of the world's largest hydropower plant in terms of energy output, is located along the border of Brazil and Paraguay (hydrological basin 4 in Fig. 1) and has a power capacity of 14,000 MW. The Sobradinho reservoir is in the southern part of Brazil's northeast region, with most of its catchment area located in central-east Brazil (basin 2 in Fig. 1). It has a total capacity of 1050 MW, but it also regulates the water flow of five more downstream run-of-river hydro plants with an aggregate capacity of 8940 MW. The Tucuruí reservoir is located in northern Brazil (basin 1 in Fig. 1) and has a total capacity of 8365 MW. Together, their power capacity represents about 46% of the total hydroenergy capacity installed in Brazil. Peak inflows to these reservoirs usually occur between January and March.

The left panel in Fig. 11 shows the r^2 score for these three reservoirs as a function of lead time of forecast and model used. For all three reservoirs, the use of climate predictors has improved forecast skills. For the Itaipu reservoir (top panel), improvements in forecasts are obtained up to 6 month lead when the RIDGE model was used. For Sobradinho and Tucuruí, better forecasts are limited to three and two leads, respectively.

A detailed look at the RIDGE model r^2 score as a function of forecast month and lag time of predictors shows (right panels in Fig. 11) interesting results. Forecast skills are seasonally varying, with better skills during the dry months (July–October). February and March (wettest months) flows in Itaipu (top right panel in Fig. 11) are only predictable at leads 5 and 6 months. On the other hand, forecasts made for the February and March flows of Sobradinho (middle right panel in Fig. 11) show moderate skills up to 3 month lead with a recovering in the skill at 5 and 6 month lead times. February streamflow forecasts for the Tucuruí reservoir (bottom right panel in Fig. 11) shows a drop in the skill from 2 month lead. As the dry season approaches, the drop in the forecast skill tends to occur at longer leads.

Correlations between model forecasts and observed values of streamflow for the three reservoirs are shown in Fig. 12. The high

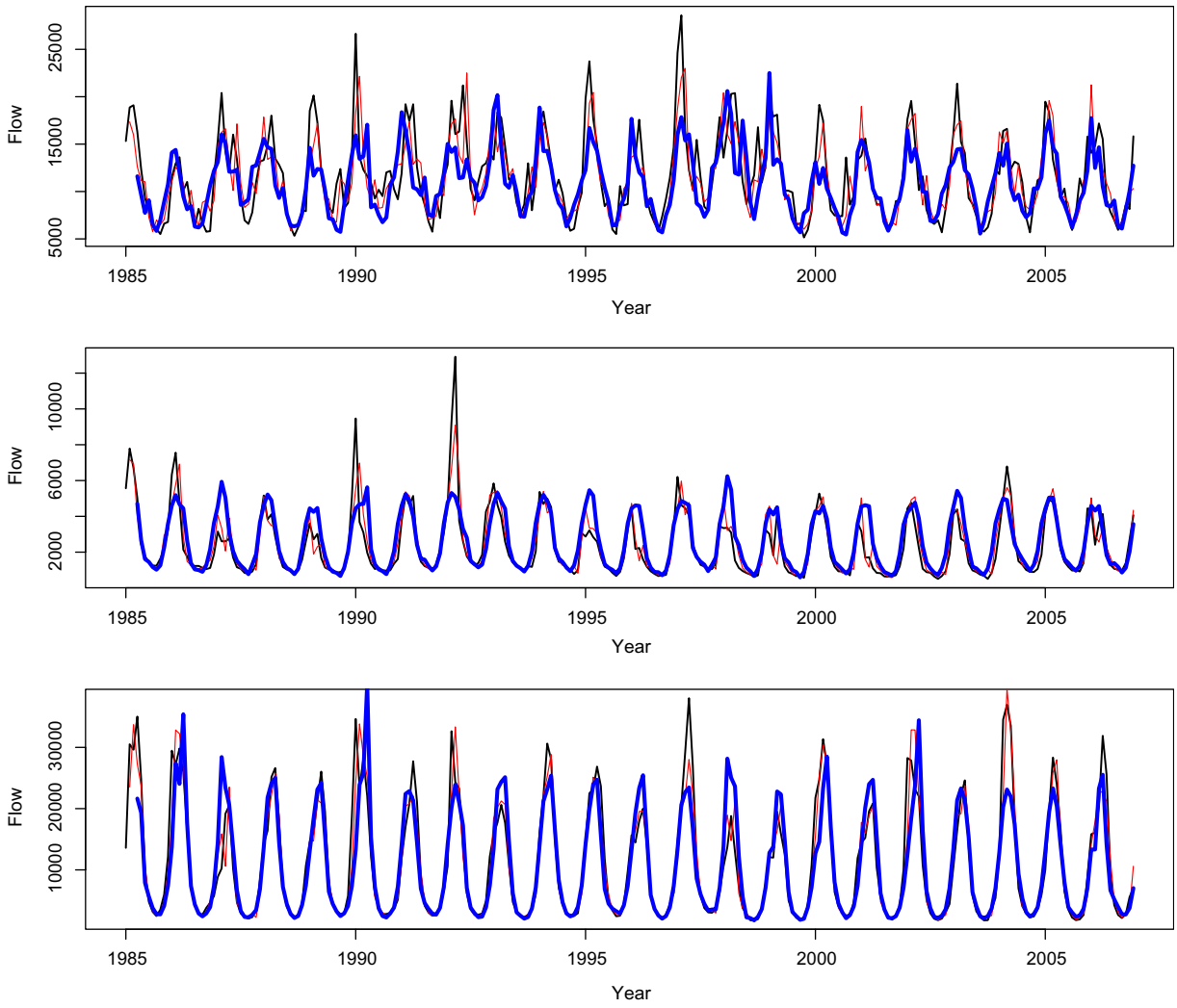

Fig. 13. Observed streamflow (black lines), 1 month (red lines) and 2 month (blue lines) lead time forecasts from the RIDGE model for Itaipu (top), Sobradinho (middle) and Tucuruí (bottom) hydropower reservoirs.

correlations on the left panels suggest that the forecasts tend to follow the seasonal cycle of the observed streamflow. The seasonal dependence of the forecast skill observed for the r^2 score is also evident for the correlation skill, in particular for the Sobradinho and Tucuruí forecasts. Statistically significant correlations for Itaipu appear up to 2 month lead for May to July forecasts and up to 6 months for the October to December forecasts. A partial recovering in the correlation skill is also observed for the February to April forecasts.

Finally, Fig. 13 shows, for these three reservoirs, 1 and 3 month lead time forecasts from the RIDGE model. The seasonal cycle and low flows are skilfully predicted at these leads for all three reservoirs. High flows are better predicted at 1 and 2 (not shown here) month leads.

Skill recovery

The convex curve observed for the skills of the RIDGE and PARX models (Figs. 7, 9 and top panel in Figs. 11 and 12) suggest that some forecasts could become more accurate as the lead time increases. Although it seems paradoxical, a decline and a subsequent recovery in the forecast skills as lead time increases it is not new in the literature (e.g. Lau and Chang, 1992; Balmaseda et al., 1995; Eckel and Walters, 1998; Xue et al., 2000). In fact, the climate predictors used in Eq. (2) play different roles on the streamflow process at different lag times. For instance, Fig. 14 shows lagged correlations between the January inflow of the Itaipu reservoir and the three climate predictors used in Eq. (2). Note that while the NINO3 correlation curve (red line in Fig. 14) decreases as the lead time increases, the correlation with the south Atlantic SST (blue line in Fig. 14) achieves its maximum value at 4 month lag time. Differently from these two curves, the low-level zonal wind correlation curve (black line in Fig. 14) changes its sign and achieves maximum absolute values at 1 month and 4 month lags. Hence, as in Eq. (2) the lag time τ is the same as the lead time of the forecast, i.e., a 3 month lead time forecast means that ones uses the climate predictors lagged by 3 months ($\tau = 3$, though it is possible to use any $\tau \geqslant 3$ for a 3 month lead forecast), it is expected that the climate indexes at 4 month lag will be better predictors for the January flow than those indexes at 3 month lag. This is more evident in the right top panel of Fig. 11, which shows a drop in the r^2 score when forecasting the January inflow of Itaipu at 3 month lead time.

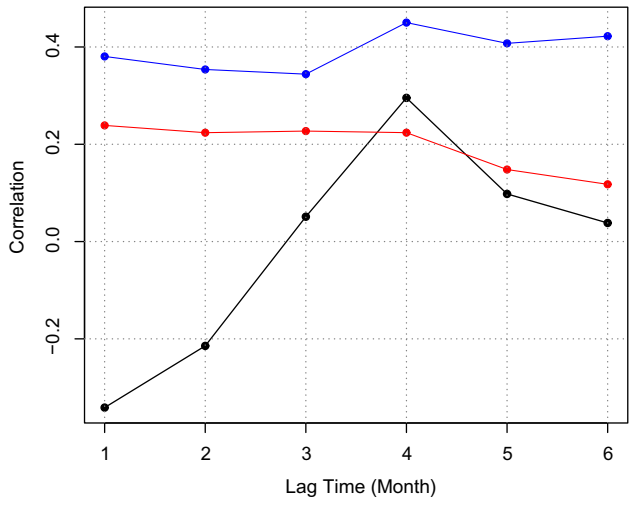

Fig. 14. Lagged correlations between the January inflow of the Itaipu reservoir and the low-level zonal wind (black line), NINO3 (red line) and south Atlantic SST (blue line) indexes.

Conclusion

Inclusion of climate information into monthly streamflow forecasts using a periodic-auto-regressive model was shown to improve the ability to forecast streamflow for the Brazilian Hydro system. The indexes used in this work are from the tropical Pacific and sub-tropical Atlantic SST and from the low-level zonal wind over southeastern Brazil. The forecast models are built using two different methodologies: (i) classical linear regression with best set of climate predictors selected by the BIC criterion and (ii) ridge regression on the full set of predictors. Having the constant periodic mean as a benchmark model, we use the r^2 score to compare model skills. Correlation analysis are also used to assess model performances. It is possible that nonlinear relations between potential climate predictors and streamflow in the region exist. One could try to identify such predictors and formulate a nonlinear regression model. Ideally, the predictors would still be selected using known physical relationships or efforts to assess the possible physical link have to be made. In the context of a seasonally varying model the number of models and parameters to be estimated and compared would be very large. Consequently, in this paper we focused on a simple extension of the existing PAR model and demonstrated the potential utility of adding climate information.

The results show that climate indices are able to increase the predictability of streamflows up to 3 month lead times for most reservoirs. However, large basin reservoirs tend to have higher skills, which is somehow expected, given that flows from large catchments are less sensitive to local events of rainfall and thus respond better to large-scale climate forcings. Forecast skills are also seasonally dependent, with reduced skills within the wet period. In terms of modeling, the RIDGE regression model has the best skills, especially for 2 and 3 month leads.

The ridge regression model proposed in this work requires the estimation of a few parameters. It can be adapted easily for real time streamflow forecasts, since the climate predictor data are constantly updated and made available on a regular basis. Future research should focus on a better modeling of the parameter uncertainties, which were not fully considered here. For instance, a Bayesian framework could be used to estimate the model parameters in place of the ridge regression. The recovery in the skill observed for Itaipu forecasts during the wet months suggests that longer lag predictors may be more important than short lag predictors in terms of model accuracy. Hence a more careful selection of lag times of predictors should be explored. For instance, the lead time of the forecast does not need to be the same as the predictors' lag. Individual, at site correlation analysis should also be investigated in order to obtain better climate predictors. Finally, given that the models developed here have established a correspondence between hydropower flows and climate variability, the potential impacts of global climate change on hydropower generation in Brazil can be evaluated using simulations (from IPCC scenarios, for instance) of the tropical Pacific SST, sub-tropical Atlantic SST and low-level zonal wind and posterior computation of streamflows scenarios.

Acknowledgment

Supported by Fulbright and CAPES (Brazil) through Grant # 1650-041.

References

Balmaseda, M.A., Davey, M.K., Anderson, D.L.T., 1995. Decadal and seasonal dependence of ENSO prediction skill. Journal of Climate 8, 2705–2715.

Barros, M.T.L., Tsai, F.T.-C., Yang, S.-L., Lopes, J.E.G., Yeh, W.W.-G., 2003. Optimization of large-scale hydropower system operations. Journal of Water Resources Planning Management 1290 (3), 178–188.

Barros, V., Gonzalez, M., Liebmann, B., Camilloni, I., 2000. Influence of the south Atlantic convergence zone and south Atlantic Sea surface temperature on interannual summer rainfall variability in southeastern South America. Theoretical and Applied Climatology 67, 123–133.
Berbery, E.H., Collini, E.A., 2000. Springtime precipitation and water vapor flux over southeastern South America. Monthly Weather Review 128, 1328–1346.
Cardoso, A.O., Dias, P.L.S., 2006. The relationship between ENSO and Paraná River Flow. Advances in Geosciences 6, 189–193.
Carvalho, L.M.V., Jones, C., Liebmann, B., 2004. The south atlantic convergence zone: intensity, form, persistence, and relationships with intraseasonal to interannual activity and extreme rainfall. Journal of Climate 17, 88–108.
Cataldi, M., Machado, C.O., Guilhon, L.G.F., Chou, S.C., Gomes, J.L., Bustamante, J.F., 2007. Analysis of rainfall forecasts from ETA model as input to streamflow weekly forecasts. In: I ONS Workshop of Streamflow Forecasts (in Portuguese).
Coelho, C.A.S., Uvo, C.B., Ambrizzi, T., 2002. Exploring the impacts of the tropical pacific SST on the precipitation patterns over South America during ENSO periods. Theoretical and Applied Climatology 71, 185–197.
Collischonn, W., Haas, R., Andreolli, I., Tucci, C.E.M., 2005. Forecasting river uruguay flow using rainfall forecasts from a regional weather-prediction model. Journal of Hydrology 305, 87–98.
Costa, F.S., Damázio, J.M., Maceira, M.E.P., Denício, M., Guilhon, L.G., Silva, S.B., 2003. Stochastic model of monthly streamflow forecast – PREVIVAZM. In: XV Brazilian Simposium of Water Resources (in Portuguese).
Costa, F.S., Maceira, M.E.P., Damázio, J.M., 2007. Hydrological forecast models applied to planning and operation of the Brazilian hydropower system. In: I ONS Workshop of Streamflow Forecasts (in Portuguese).
Diaz, H., Markgraf, V., 2000. El Niño and the Southern Oscillation : Multiscale Variability and Global and Regional Impacts. Cambridge University Press.
Diebold, F.X., Mariano, R., 1995. Comparing predictive accuracy. Journal of Business and Economic Statistics 13, 253–265.
Eckel, F.A., Walters, M.K., 1998. Calibrated probabilistic quantitative precipitation forecasts based on the MRF ensemble. Weather and Forecasting 13, 1132–1147.
Figueroa, S.N., Satyamurty, P., da Siva Dias, P.L., 1995. Simulations of the summer circulation over the South American region with an eta coordinate model. Journal of the Atmospheric Sciences 52 (10), 1573–1584.
Filho, F.A.S., Lall, U., 2003. Seasonal to interannual ensemble streamflow forecasts for Ceara, Brazil: applications of a multivariate, semiparametric algorithm. Water Resources Research 39 (11).
Gomide, F.L.S., 2004. Hydropower development in Brazil: experiences and perspectives. In: United Nations Symposium on Hydropower and Sustainable Development, Beijing, China.
Grantz, K., Rajagopalan, B., Clark, M., Zagona, E., 2005. A technique for incorporating large scale climate information in basin-scale ensemble streamflow forecasts. Water Resources Research, 41.
Grimm, A.M., 2003. The El Niño impact on the summer monsoon in brazil: regional processes versus remote influences. Journal of Climate 16, 263–280.
Grimm, A.M., 2004. How do La Niña events disturb the summer monsoon system in Brazil? Climate Dynamics 22, 123–138.
Grimm, A.M., Barros, V.R., Doyle, M.E., 2000. Climate variability in southern South America associated with El Niño and La Niña events. Journal of Climate 13, 35–58.
Grimm, A.M., Ferraz, S.E.T., Gomes, J., 1998. Precipitation anomalies in southern Brazil associated with El Niño and La Niña events. Journal of Climate 11, 2863–2880.
Guilhon, L.G.F., Rocha, V.F., Moreira, J.C., 2007. Comparison of hydropower inflow forecast models. In: I ONS Workshop of Streamflow Forecasts (in Portuguese).
Hastenrath, S., 1994. Climate Dynamics of the Tropics. Kluwer Academic Publisher.
Hastie, T., Tibshirani, R., Friedman, J., 2001. The Elements of Statistical Learning. Springer.
Kaplan, A., Cane, M., Kushnir, Y., Clement, A., Blumenthal, M., Rajagopalan, B., 1998. Analyses of global sea surface temperature 1856–1991. Journal of Geophysical Research 103 (18), 518–567. 589.
Kelman, J., Vieira, A.M., Rodriguez-Amaya, J.E., 2000. El niño influence on streamflow forecasting. Stochastic Environmental Research and Risk Assessment 14, 123–138.
Kumar, D.N., Maity, R., 2008. Bayesian dynamic modelling for nonstationary hydroclimatic time series forecasting along with uncertainty quantification. Hydrological Processes 22, 3488–3499.
Lau, K.-M., Chang, F.C., 1992. Tropical intraseasonal oscillation and its prediction by the NMC operational model. Journal of Climate 5, 1365–1378.
Lenters, J., Cook, K.H., 1995. Simulation and diagnosis of the regional summertime precipitation climatology of South America. Journal of Climate 8, 2988–3005.
Liebmann, B., Kiladis, G.N., Marengo, J.A., Ambrizzi, T., Glick, J., 1999. Submonthly convective variability over South America and the south Atlantic convergence zone. Journal of Climate 12, 1877–1891.
Lima, C., Lall, U. Filho, F.A.S., 2006. Influences of ENSO events on the hydropower production in Brazil. In: Eos Trans. AGU, vol. 87(52) (Fall Meet. Suppl., Abstract H44A-02).
Lima, C.H.R., Lall, U., 2008. Flood hydroclimatology: extreme events, non-stationarity, large scale climate processes and a perspective for simulations under global climate changes. In: II South-southeast Symposium of Water Resources. Brazilian Association of Water Resources, Rio de Janeiro (in Portuguese).
Lima, C.H.R., Lall, U., Filho, F.A.S., 2007. Variability and climate teleconnections associated with the natural inflows of the Brazilian hydropower system. In: XVII Brazilian Symposium of Water Resources (in Portuguese).
Maceira, M.E.P., Penna, D.D.J., Damázio, J.M., 2005. Synthetic generation of energy and streamflow scenarios for the energetic operation planning. In: XVI Brazilian Simposium of Water Resources (in Portuguese).
Maity, R., Kumar, D.N., 2008. Basin-scale stream-flow forecasting using the information of large-scale atmospheric circulation phenomena. Hydrological Processes 22, 643–650.
Marreco, J.M., Carpio, L.G.T., 2006. Flexibility valuation in the Brazillia power system: a real options approach. Energy Policy 34, 3749–3756.
Moura, A.D., Shukla, L., 1981. On the dynamics of droughts in northeast Brazil: observations, theory and numerical experiments with a general circulation model. Journal of the Atmospheric Science 38, 2653–2675.
Nogués-Paegle, J., Mo, K.C., 1997. Alternating wet and dry condition over South America during summer. Monthly Weather Review 125, 279–291.
ONS, 2007. Streamflow Series Update – 1931–2006 period (in Portuguese). Tech. Rep., Natural Operator of the Electrical System.
Reynolds, R.W., Smith, T.M., 1994. Improved global sea surface temperature analyses using optimum interpolation. Journal of Climate 7, 929–948.
Ropelewski, C.F., Halpert, M.S., 1987. Global and regional scale precipitation patterns associated with the el niño/southern oscillation. Monthly Weather Review 115, 1606–1626.
Silva, B.C., Collischonn, W., Tucci, C.E., Clarke, R.T., Corbo, M.D., 2007. Short term streamflow hydroclimatic forecast for the São Francisco Basin. In: I ONS Workshop of Streamflow Forecasts (in Portuguese).
Uvo, C.B., Graham, N.E., 1998. Seasonal runoff forecast for northern South America: a statistical model. Water Resources Research 34 (12), 3515–3524.
Vera, C., Baez, J., Douglas, M., Emmanuel, C.B., Marengo, J., Meitin, J., Nicolini, M., Nogues-Paegle, J., Paegle, J., Penalba, O., Salio, P., Saulo, C., Dias, M.A.S., Dias, P.S., Zipser, E., 2006. The South American low-level jet experiment. Bulletin American Meteorological Society 87, 63–77.
Xue, Y., Leetmaa, A., Ji, M., 2000. ENSO prediction with markov models: the impact of sea level. Journal of Climate 13, 849–871.